Automated facial landmark detection, comparison and visualization

Marek Galvánek Katarína Furmanová Igor Chalás* Jiří Sochor
Faculty of Informatics, Masaryk University

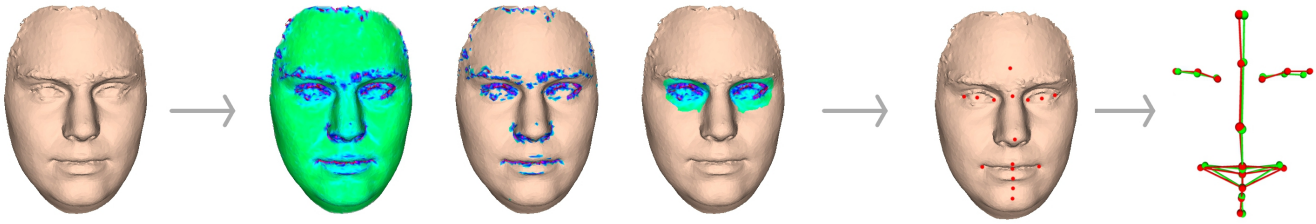

Figure 1: Workflow of our system. Our system takes as an input 3D facial model and uses registration and segmentation for detection of landmarks. The landmarks are further processed by comparative algorithm and the results are visualized.

Abstract

Anthropometric facial landmarks and their detection has wide application in anthropology and forensic science. More specifically, these landmarks play an important role in facial comparison, in the analysis of morphological changes during human growth and in searching for the variability of human faces (e.g., sexual dimorphism). The automatic extraction of landmarks is a challenging area and specific visualization methods serving for the comparison are crucial for the correct interpretation of the results. In this paper we introduce a novel system which incorporates a newly proposed algorithm for automatic landmark detection. The algorithm is based on surface curvature and symmetric profile extraction. The landmarks are then used in the Generalized Procrustes analysis for facial comparison. Our system also introduces appropriate visualization methods supporting the presentation and understandability of the results.

CR Categories: I.4.6 [Image Processing And Computer Vision]: Segmentation—Edge and feature detection; I.4.7 [Image Processing And Computer Vision]: Feature Measurement—size and shape;

Keywords: facial landmark detection, Procrustes analysis, facial comparison, facial comparison visualization

1 Introduction

A facial landmark is a point which all faces share and has a particular biological meaning. [Dryden and Mardia 1998] sort landmarks into the four categories: *anatomical landmarks*, *mathematical landmarks*, *pseudo-landmarks* and *labeled landmarks*. In this paper we are interested in anatomical landmarks that correspond between organisms in some biologically meaningful way (e.g., the corner of an eye).

A study which uses facial landmarks is called facial morphology. Among its numerous objectives we can find analysis of facial abnormalities, dysmorphologies, growth changes, esthetical aspects or purely theoretical research of facial anthropology. Moreover, facial landmarks play prominent role in applications of computer science such as facial recognition, animation, expression analysis, facial reconstruction, tracking, gesture understanding, surveillance system, lip reading, sign language interpretation and much more.

Manual landmarking is time consuming and lengthy, therefore automatic detectors are very useful. However, automated landmarking has to overcome many challenges such as artifacts created during 3D image acquisition (especially true for area of eyes and facial hair), non-uniform facial expressions and positions and occlusions of facial features. Another issue is structural dependency of landmarks, i.e., one landmark is defined by other landmarks. Nevertheless, there exist lot of approaches based on different input data and techniques (more in Section 2).

There are many methods available for facial comparison, differing mainly in the type of features they process (outline-based, landmark-based, surface-based, etc.). When it comes to landmark-based methods, Bookstein's shape coordinates [Bookstein 1986] and Procrustes analysis [Gower 1975] are most widely used techniques. Unfortunately, without further processing with statistical methods such as Principal components analysis (PCA) or Canonical Variates Analysis (CVA), its results give little information. However, appropriate visualisation and visual analysis can help with uncovering relationships, data validation or hypothesis formulation.

Comparative visualization concentrates on the visual appearance and presentation of differences and similarities in two or more datasets [Pagendarm and Post 1995]. According to [Gleicher et al. 2011] there are three main approaches to visual data comparison: juxtaposition, superposition and explicit encoding. Juxtaposition is the simplest method, which positions the meshes next to each other. Thus, it is not suitable for comparing larger sets of data. The superposition approach is used to place objects one on top of the other and presenting them in the same time and space. The explicit encoding depicts the relationship between objects by encoding visually.

*e-mail: chalas@fi.muni.cz, author for correspondence

SCCG 2015, April 22 – 24, 2015, Smolenice, Slovakia.

ACM 978-1-4503-3693-2/15/04 $15.00
http://dx.doi.org/10.1145/2788539.2788540

This paper summarizes the achievements of our current research in the area of automated facial landmark detection and their usage for facial comparison with possibility of advanced visualization.

2 Related Work

In the last years many techniques have been developed to detect facial landmarks on facial images. Historically, first approaches worked with 2D images of faces. The survey of these techniques can be found, e.g., in [Rathod et al. 2014]. With the advances in hardware equipment and image capturing, new approaches working with 2.5D and later with 3D facial data started to arise as well. These approaches have emerged as a major face recognition solution to deal with unsolved issues in 2D, e.g., lighting and pose variations [Faltemier et al. 2008].

3D landmark detectors can be divided into three main categories: approaches which are dependent on geometric information, approaches based on landmark projection from a generic model and approaches supported by trained statistical feature models. Some existing detectors use the combination of these methods as well.

Geometric features can be detected using various methods and operators. There are some landmark detectors that analyze the curvature and shape of a model [Vezzetti et al. 2013] and additionally analysis of edges can lead to even better results [Segundo et al. 2007]. Method described in [Zhang et al. 2006] introduces a symmetry profile extraction. Both surface and profile curvature are computed to locate landmarks along the symmetry profile. Similar technique uses Hough transformation to extract the symmetry profile [Li and Pedrycz 2014].

Different approaches use manually landmarked facial template. Face model is registered to the template and then the landmarks are mapped from template to the model [Whitmarsh et al. 2006]. A combined technique detects 17 landmarks by a geometric methodology. To improve the accuracy, the model can be registered to a deformable template [Liang et al. 2013]. Other approaches use a training set of manually labeled models. Landmark detector in [Nair and Cavallaro 2009] is based on the fitting model to the 3D Point Distribution Model without relying on texture and pose. Other similar techniques use local shape descriptors [Ruiz and Illingworth 2008; Perakis et al. 2011] and Gaussian curvature descriptor map [Creusot et al. 2011].

Two-dimensional techniques are also useful for 3D landmark detectors. [Erdogmus and Dugelay 2011] describe method based on 2D texture and 3D shape curvature. Technique introduced in [Bockeler and Zhou 2013] first computes 2D gradient images from a polygonal model and then detects landmarks using the Viola & Jones classifier. There are also other interesting approaches, that can be found, e.g., in comparative study by [Çeliktutan et al. 2013].

The development of new landmark extraction methods naturally leads to advances in geometric morphometrics and shape analysis approaches based on landmarks. The most prominent and widely used techniques in this area are Bookstein's shape coordinates [Bookstein 1986] and Procrustes analysis [Gower 1975]. Both methods use the superimposition principle to eliminate the non-shape variations, such as position, orientation and scale.

Bookstein's shape coordinate (also referred to as two-point coordinate) system [Bookstein 1986] is simple registration technique useful in combination with, e.g., outline-based methods and user-controlled input. However it was mostly superseded by methods based on Procrustes analysis.

Procrustes analysis (also Procrustes superimposition) and its more general version Generalised Procrustes analysis (GPA) is iterative superimposition method. It takes as an input a set of landmarks (referred to as a configuration) for each analysed object and uses least-squares fit to estimate the transformation parameters. The goal is to minimize the specimen deviations from mean configuration [Gower 1975; Rohlf and Slice 1990]. We will further discuss this method and our application of GPA in Section 4. Other variations of GPA were introduced to gain more precise results in specific fields. Generalized resistant-fit (GRF) presented in [Rohlf and Slice 1990] uses the classic GPA to achieve an initial alignment and then uses the resistant-fit method to obtain the final alignment of each object to a mean consensus object. Variations of GPA include usage of sliding semi-landmarks (points of arbitrary position along curves or shape which help to describe some specifications, e.g.,curvature) along the fixed landmarks [Bookstein 1997; Gunz et al. 2005] and account for missing landmarks [Claude 2008; Couette and White 2010; Neeser et al. 2009].

Registration methods mentioned above produce shape coordinates which describe the location of each specimen in a curved space called Kendall's shape space or its tangent space approximation. The multivariate statistical analyses of shape variation are then conducted on this data [Adams et al. 2004]. Typically one of the following methods is used to deal with the nonlinearity of landmark data: Principal components analysis (PCA), Canonical Variates Analysis (CVA), or Thin-Plate Spline method (TPS).

Appropriate visualisation of results is important for accurate understandability. In recent years, principles of interactive visual analysis were applied in scientific visualisation with great success. New outlook on the data and interactive modifications help with visual exploration and analysis of the data and contribute to the process of validating them. Case studies of some medical visualisation [Angelelli et al. 2014] and molecular visualisation [Parulek et al. 2012] tools show that linking spatial and non-spatial views on data not only helps with analysis, but could potentially lead to generation of new hypothesis.

3 Landmarks Detection

Facial landmark is an abstraction and in various papers and researches can have different meaning. We selected models of 28 individuals from The Fidentis 3D Face Database initially published in [Kotulanová et al. 2014] and and we manually determine 42 landmarks on each of them. Landmarks were determined twice by two different specialists according to the definition of facial landmarks from [Fetter 1967]. Using Procrustes ANOVA and discriminant analysis we choose 10 points, which have lowest determination error rate. We extended them by 4 biologically important points – *ektokantion* (left, right) and *cheilion* (left, right). These 14 points describe eyes, nose and mouth. Points *glabela*, *nasion*, *pronasale*, *labrale superius*, *stomion*, *labrale inferius*, *sublabiale* and *pogonion* lie along symmetry profile and points *ektokantion*, *entokantion* and *cheilion* are bilateral – pair landmarks, which lie on both sides of face. Visualized points are shown in Figure 8 and the definitions can be found in Table 1. The selected set of landmarks partially overlaps with definitions of facial feature points in MPEG-4 Face and Body Animation International Standard [ISO/IEC 2004], though we also detect biological landmarks important for forensic identification, which are not defined in this standard.

Implemented algorithm combines geometric landmark detectors based on curvature analysis [Vezzetti et al. 2013] and symmetry profile extraction [Zhang et al. 2006]. Algorithm is divided into

Name	Shorcut	Definition
Ektokantion (R, L)	EX	bilateral point located at the lateral corner of the eye where the upper and lower eyelids meet
Entokantion (R, L)	EN	bilateral point, located at the medial corner of the eye where the upper and lower eyelids meet
Glabela	G	the most forward point, located between eyebrows in the midline
Nasion	N	the most deepest point on the nasal bridge in the midline
Pronasale	PRN	the most protrusive point on the nasal tip in the midline
Labrale superius	LS	is located in the midline – between the philtral ridges – along the vermillion border of the upper lip
Stomion	STO	point, located along the labial fissure in the midline; when the lips are closed, locating *stomion* is relatively straightforward
Labrale inferius	LI	point in the midline along the inferior vermillion border of the lower lip.
Cheilion (R, L)	CH	bilateral point located in the corners of lips, where meets upper and lower lip.
Sublabiale	SL	is located at the midpoint of the labiomental groove or sulcus; *sublabiale* demarcates the inferior extent of the cutaneous lower lip
Pogonion	PG	the most forward point on the chin.

Table 1: Landmarks definition

three main parts: Face Registration, Curvature analysis and Symmetry profile extraction.

3.1 Face registration

First step is to align the face to Frankfort horizontal plane, which represent anatomical position of human skull. This plane is defined as a plane passing through the inferior margin of the left orbit and the upper margin of each ear canal or external auditory meatus, called the porion. It means, that the plane is horizontal when the position of the head is naturally oriented. This position is used to manually label facial landmarks, but we use it for automatic landmarking too. The face model is registered with the template model, which is manually positioned into Frankfort horizontal, using ICP algorithm [Besl and McKay 1992]. This algorithm rotates and translates the face model to the template until it reaches maximal number of iterations, or difference between 2 last iterations is smaller than given error rate.

3.2 Curvature analysis

In contradiction to technique in [Vezzetti et al. 2013], we use only minimal and maximal principal curvature but independently for every face feature. It means that curvature computation, noise filtering and feature segmentation is applied on a nose, eyes and mouth separately with different parameters. For curvature computation we use definition by [Meyer et al. 2003]. Discrete curvature is defined by averaging Voronoi cells and the mixed Finite-Element/Finite-Volume method.

3.2.1 Nose

The tip of the nose segment is obtained as the region with the maximum values of the minimal principal curvature. Artefacts like beard or eyelashes can impact on the final segmentation, therefore we apply linear anisotropic filter [Hildebrandt and Polthier 2004] to denoise face model. Computed principal curvature values are then thresholded via automatic threshold filter. We tried 16 automatic methods [Beare 2012; Landini] for threshold computation and the best result for nose region was reached using Triangle filter [Beare 2012]. Using the computed threshold we then chose the biggest continuous region, as nose tip region. Most forward point of segmented region (along z-axis) is *pronasale*. Whole process is shown in Figure 2.

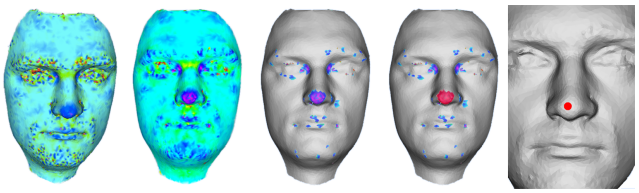

Figure 2: From left: original image with minimal curvature, anisotropic linear filter, thresholded values, nose tip segmentation, landmark detection

3.2.2 Mouth

Segmentation of mouth region is similar to nose segmentation. First the face is smoothed to remove artifacts. In this case we used anisotropic non-linear filter [Hildebrandt and Polthier 2004] to prevent sharp edges – lips and labial fissure. The best threshold results were reached using Renyi Entropy method [Beare 2012]. We find mouth region as the biggest continuous segment under (y-axis) already located landmark *pronasale*. Since the face is already registered to Frankfort horizontal plane, we can take this condition into account (Section 3.1). Left and right point *cheilion* are then extract as leftmost and rightmost points of segmented region along y-axis. Point *stomion* is located between *cheilion* points with x coordinate same as *pronasale*. This is only an approximated location of *stomion* and will be specified in Section 3.3. Mouth segmentation is shown in Figure 3.

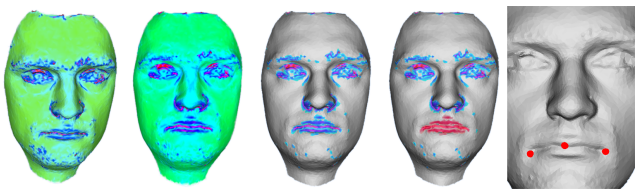

Figure 3: From left: original image with maximal curvature, anisotropic non-linear filter, thresholded values, mouth segmentation, landmarks detection

3.2.3 Eyes

In contrast to previous segmentations, eyes segments are more accurate without any denoising and smoothing. In some tested faces

denoising removed some features of eyes and results are inaccurate. This time we use Max Entropy [Beare 2012] threshold method. Eye segments are chosen as biggest continuous regions above *pronasale y* coordinate and to left/right from *pronasale x* coordinate. Left/right *ektokantion* and left/right *entokantion* are detected as the most left/right vertices of eyes regions. Eyes processing is shown in Figure 4.

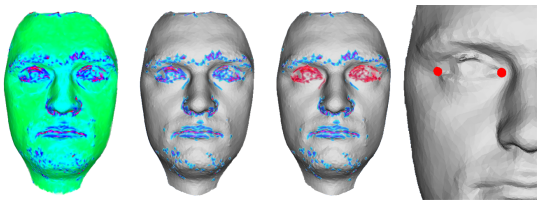

Figure 4: From left: original image with maximal curvature, thresholded values, eyes segmentation, landmarks detection

3.3 Symmetry Profile

After curvature analysis of model, we detected 8 facial landmarks using symmetry profile extraction. 2 of them are points already located by curvature analysis, which lie on facial midline and we only refine their position. We also detect 6 new points. Method for symmetry profile extraction is taken from [Zhang et al. 2006]. Face model is first mirrored along x-axis. Original and mirrored faces are then registered using ICP algorithm (already used in Registration phase – Section 3.1). Symmetry plane is then easily determined as mean value of distance for every point p and its mirror p'. The symmetry profile of a face is extracted by intersecting the symmetry plane with the facial surface. To analyse the symmetry profile we compute curvature of 2D curve. First, the symmetry profile is interpolated to a parametric 2D spline function and then we compute curvature using osculating circle method [Weisstein]. Points we detect are all located on peaks or valleys of a curve – points with maximal or minimal values of a curvature. To extract these points we used morphological operator [Soille 2003], which determine depth or dynamic of each extremum of a curve. Then we choose 5 maxima with highest dynamics (*glabela*, *pronasale*, *labrale superius*, *labrale inferius* and *pogonion*) and 3 minima with highest dynamics (*nasion*, *stomion* and *sublabiale*). Process of symmetry profile extraction and analysis is illustrated in Figure 5.

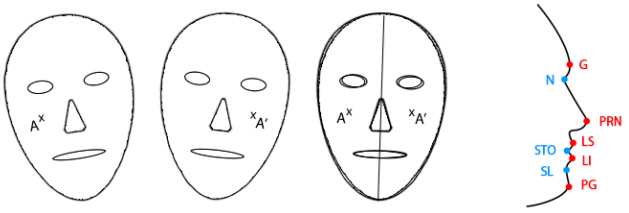

Figure 5: From left: original image, mirrored image, registered images and symmetry profil extraction, detected landmarks on symmetry profile (red: local maxima, blue: local minima)

4 Procrustes analysis and visualisation

After the facial landmark abstraction we use either basic Procrustes analysis (for 2 faces) or its generalized version, GPA (for set of faces), in order to align models. As stated in Section 2, Procrustes analysis is a superimposition method used to eliminate non-shape variations from the specimen by shape-preserving transformations – translation, rotation and scaling. Since our working set of landmarks is of same cardinality for each specimen we use the basic implementation described in [Gower 1975]. The algorithm iteratively computes approximate mean configuration (AMC) and centroid of each configuration, then translates the centroids to the origin of coordinate system and aligns the configurations to the AMC. After each iteration new AMC is computed. The algorithm stops when the the AMCs in last two iterations match – i.e. the true mean configuration is found. Numerical results of our comparison methods are based on Procrustes distance, which is approximately the square root of the sum of squared differences between the positions of the landmarks in two superimposed configurations [Marcus 1996]. However, since Procrustes distance is a single number, it doesn't give us any information about local variations and differences. That's why it is important to employ interactive visualisation in our system. Moreover, in our system we support three specific modules of comparison: pairwise facial comparison (module 1:1), comparison of one face against selected set of faces i. e., database (module 1:N) and comparison of set of faces among themselves (module N:N). Each of these modules has different aim. We adjusted the comparison process to gain desired results for each module and for each situation we created context-dependent visualisation. For better visualisation results we also interpolate another landmark called *pupila* (P) as a mean position of *entokantion* and *ektokantion*.

4.1 Pair comparison (1:1)

The goal the method is to determine how close are two models related, or optionally, to determine whether the facial models depict the same person. However, it is impossible to percentually state how closely are the two models related based on the Procrustes distance only. To give statistical background to the results we introduced a possibility to use reference database. The user can choose precomputed database of 150 specimens, where landmarks were manually selected by experienced scientists (the risk of erroneous calculation due to misplaced landmark is thus limited). Alternatively, we offer possibility to use user defined precomputed database (which may be exported from the N:N module) or compute the database at runtime from selected models. This gives us ability to compare the computed Procrustes distance of given pair with distances in database and set the percentile placement within database – i.e., we gain information how closely are the two specimens matched in relation to database (Table 2).

Minimal distance in database	2.3797
Maximal distance in database	43.0604
Average distance in database	14.4397
Procrustes distance of selected models	9.0009
Percentile in database	82.6045

Table 2: Example of numerical results of pair comparison

To show the local differences between the two models we constructed a visualisation which consists of registered landmark configurations. To provide better shape description we connected closely related points (mouth, eyes and medial plane) and overlaid these wired models of two faces. Our system works with 3D data and allows manipulation with the model (camera translations, rotation, etc.), however if the two models are closely related, the small differences may not be visible. Therefore we introduced interactive

method to enhance these differences. The distance between two points A and B is enhanced in following way:

$$\begin{aligned} v &= A - B \\ A &= A + v \cdot k \\ B &= B - v \cdot k \end{aligned}$$

where k is interactively adjustable coefficient. This simple method provides means to visually analyze even small local differences. Unfortunately, the downside of this method is distortion of original facial shape (Figure 6).

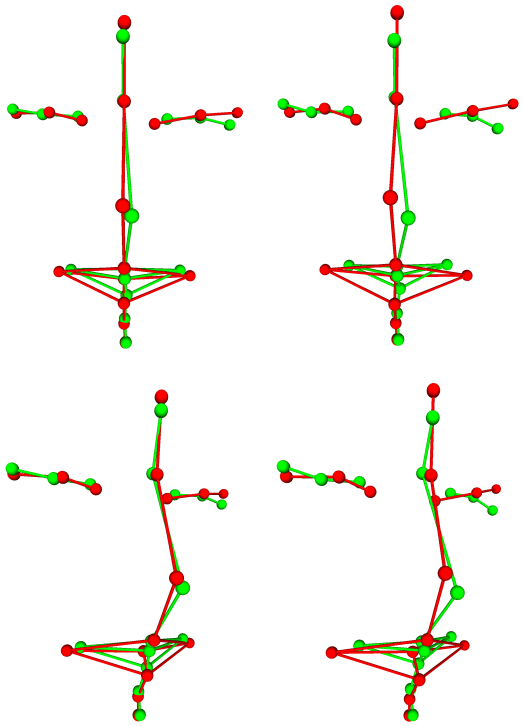

Figure 6: Pair comparison visualisation – frontal (top) and peripheral (bottom) view of basic configurations (left) and enhanced distances (right)

4.2 Comparison with database (1:N)

When comparing one model with database, first a reference model is selected, then the landmark configuration of this reference model is used as base for Procrustes analysis and all configurations from database are aligned to the reference configuration. Procrustes distance between reference model and each model in database is used as numerical results of Procrustes analysis – a vector of n values, where n is the number of entries in database. This is useful for finding the closest match in database (e.g. comparing a model of suspect with database of criminals). Also a table with basic statistical information similar to (Table 2) giving minimal, maximal and average distance in set can be derived. Sometimes it is also desired to analyse in what aspects the individual differs from given group. For this purpose we designed visualisation which shows deviation between database and reference model for each landmark. Mean configuration of database, computed during Procrustes analysis, is displayed and for each landmark a vector (visualised as an arrow) is drawn to show the deviation of reference configuration from the mean configuration (Figure 7). Again we use the interactive enhancement, this time, however, we only enhance the deviation vector. The position of reference configuration is fixed to preserve the shape.

4.3 Batch processing (N:N)

Batch processing, or pair-wise comparison of set of models, is useful for database analysis. We use Generalized Procrustes analysis, where the numerical results are represented as diagonally symmetrical matrix of $n \times n$ dimension, where n is the number of entries in the database. These data can be exported and further processed by other statistical methods, e.g. PCA, or it can be used as reference database in pair comparison mode. Again, we provide basic statistical information.

To visualise the results of the comparison we highlight the mean configuration computed in GPA and draw mean wired facial model as described in Section 4.1. We also display the distribution of configurations from database, again using interactive enhancement of their distance from mean configuration (Figure 7). Additionally, we allow highlighting of configurations by selection of adherent landmark. Visual analysis of distribution of landmarks can help identifying specimen that locally significantly differ from mean or it can lead to identification of misplaced landmarks.

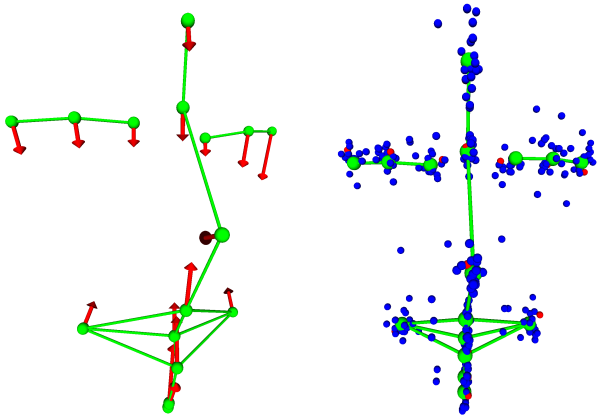

Figure 7: (left) Visual results of 1:N comparison. Red arrows show deviation of reference configuration from database. By the direction of arrows we can assume the reference model was smaller than average and had eyes placed significantly lower. (right) Results of N:N comparison. Green structure shows mean configuration. Blue landmarks show aligned configurations. Selected configuration is highlighted by red. The scattered points in the middle area likely indicate misplaced landmarks.

5 Results

Our implemented algorithm for detecting landmarks places landmarks in expected location. To verify our results we compared them with images manually labeled by experienced scientists (see Figure 8). Landmarks with worst error rate were the ones located in area of eyes – *entokantion* and *ektokantion*, followed by landmarks in mouth area. Wrong detection is often caused by notable eyelashes (especially in case of women), and by beard (in case of men).

Other landmarks are generally detected with deviation of less than 5 mm. The algorithm was optimized for meshes of minimum 5,000 vertices. For bigger meshes, the precision of the algorithm doesn't notably change, however for smaller meshes we cannot guarantee accurate results.

Presented methods were implemented as a part of FIDENTIS Analyst – forensic facial identification software available at `http://fidentis.cz`. The software includes other facial registration and comparison methods and allows combination of landmark-based registration with surface based comparison. All techniques described in this paper have been implemented in programing language Java using graphics library OpenGL. The application was tested for performance on a machine with an Intel Core i5 Quad-core 2.27 GHz CPU, 4 GB of RAM and an ATI Mobility Radeon HD 5650 graphics card. All data used for testing were gained by Vectra M1 3D imaging system and resized for purposes of testing. A comparison of the computation times and during the landmark detection on meshes of various size can be found in Table 3. It should be noted that the majority of calculation time is spent by the registration processes due to time consuming ICP algorithm.

Mesh size (vertices)	Registr. average face	Registr. mirrored face	Land-marks detection	**Total time**
2,500	2.81 s	1.54 s	1.11 s	5.46 s
5,173	5.05 s	3.74 s	1.76 s	10.55 s
39,468	30.91s	72.02 s	8.67 s	111.60 s

Table 3: Computation times of detection of 14 landmarks according to mesh size.

6 Conclusion

In this paper we presented a system which incorporates a newly proposed algorithm for automatic landmark detection. Our three-step algorithm works by positioning models into Frankfort horizontal plane, then combining surface curvature analysis and symmetric profile extraction to detect 14 facial landmarks. The landmarks are then processed by Procrustes analysis for facial registration and comparison. Our system also introduces appropriate visualization methods we devised for three different use-cases of facial comparison systems – pairwise comparison, comparison of one individual against database and batch processing of database. In the near future we would like to extend our system with another curvature operator from [Vezzetti et al. 2013], which will accurately detected landmarks with high error rate (*ektokantion*, *entokantion*). We also want to add possibility to landmarking by 2D texture of a model and change registering method. Another feature we would like to add, is manual addition and removal of landmarks – we already support manual refinement of position of detected landmarks. Since manual editing of the number of landmarks could lead to non-uniform structure of landmark configurations used in Procrustes analysis, extending our system with methods accounting for missing landmarks would be beneficial. Possible improvement of current state concerning accuracy of registration could be also introduction of semilandmarks to our system. To enrich the visual analysis, we would like to automate identification of possibly erroneous landmarks and configurations and simplify process of filtering such landmarks and configurations.

7 Acknowledgment

This work was supported by the Masaryk University Faculty of Informatics Dean's Programme (project identification MUNI/33/20/2013).

References

ADAMS, D. C., ROHLF, F. J., AND SLICE, D. E. 2004. Geometric morphometrics: ten years of progress following the revolution. *Italian Journal of Zoology 71*, 1, 5–16.

ANGELELLI, P., OELTZE, S., TURKAY, C., HAASZ, J., HODNELAND, E., LUNDERVOLD, A., PREIM, B., AND HAUSER, H. 2014. Interactive visual analysis of heterogeneous cohort study data.

BEARE, R., 2012. Histogram-based thresholding. `http://www.kitware.com/source/home/post/54`. Accessed: 2015-02-14.

BESL, P. J., AND MCKAY, N. D. 1992. Method for registration of 3-D shapes. In *Robotics-DL tentative*, International Society for Optics and Photonics, 586–606.

BOCKELER, M., AND ZHOU, X. 2013. An efficient 3D facial landmark detection algorithm with haar-like features and anthropometric constraints. In *Biometrics Special Interest Group (BIOSIG), 2013 International Conference of the*, IEEE, 1–8.

BOOKSTEIN, F. L. 1986. Size and shape spaces for landmark data in two dimensions. *Statistical Science*, 181–222.

BOOKSTEIN, F. L. 1997. Landmark methods for forms without landmarks: morphometrics of group differences in outline shape. *Medical image analysis 1*, 3, 225–243.

ÇELIKTUTAN, O., ULUKAYA, S., AND SANKUR, B. 2013. A comparative study of face landmarking techniques. *EURASIP Journal on Image and Video Processing 2013*, 1, 13.

CLAUDE, J. 2008. *Morphometrics with R*. Springer Science & Business Media.

COUETTE, S., AND WHITE, J. 2010. 3D geometric morphometrics and missing-data. Can extant taxa give clues for the analysis of fossil primates? *Comptes Rendus Palevol 9*, 6, 423–433.

CREUSOT, C., PEARS, N., AND AUSTIN, J. 2011. Automatic keypoint detection on 3D faces using a dictionary of local shapes. In *3D Imaging, Modeling, Processing, Visualization and Transmission (3DIMPVT), 2011 International Conference on*, IEEE, 204–211.

DRYDEN, I. L., AND MARDIA, K. V. 1998. *Statistical shape analysis*, vol. 4. Wiley Chichester.

ERDOGMUS, N., AND DUGELAY, J.-L. 2011. Automatic extraction of facial interest points based on 2D and 3D data. In *IS&T/SPIE Electronic Imaging*, International Society for Optics and Photonics, 78640O–78640O.

FALTEMIER, T. C., BOWYER, K. W., AND FLYNN, P. J. 2008. Rotated profile signatures for robust 3D feature detection. In *Automatic Face & Gesture Recognition, 2008. FG'08. 8th IEEE International Conference on*, IEEE, 1–7.

FETTER, V. 1967. Antropologie. Academia, Praha.

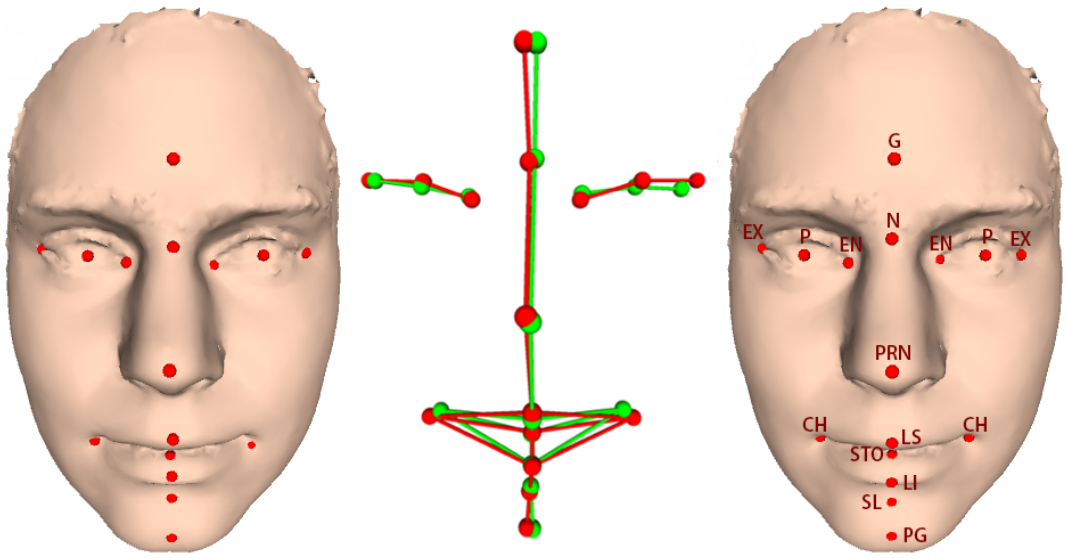

Figure 8: Comparison between landmarks detected by our algorithm (left) and manually placed landmarks (right)

GLEICHER, M., ALBERS, D., WALKER, R., JUSUFI, I., HANSEN, C. D., AND ROBERTS, J. C. 2011. Visual comparison for information visualization. *Information Visualization 10*, 4, 289–309.

GOWER, J. C. 1975. Generalized procrustes analysis. *Psychometrika 40*, 1, 33–51.

GUNZ, P., MITTEROECKER, P., AND BOOKSTEIN, F. L. 2005. Semilandmarks in three dimensions. In *Modern morphometrics in physical anthropology*. Springer, 73–98.

HILDEBRANDT, K., AND POLTHIER, K. 2004. Anisotropic filtering of non-linear surface features. In *Computer Graphics Forum*, vol. 23, Wiley Online Library, 391–400.

ISO/IEC. 2004. Information technology – coding of audio-visual objects – part 2: Visual. ISO/IEC 14496-2.

KOTULANOVÁ, Z., CHALÁS, I., AND URBANOVÁ, P. 2014. 3D virtual model database of human faces: Applications in anthropology and forensic sciences. In *Mikulov Anthropology Meeting. The Dolní Věstonice Studies 20*, Academy of Sciences of the Czech Republic, Brno, 177–180.

LANDINI, G. Auto threshold. `http://fiji.sc/Auto_Threshold`. Accessed: 2015-02-14.

LI, D., AND PEDRYCZ, W. 2014. A central profile-based 3D face pose estimation. *Pattern Recognition 47*, 2, 525–534.

LIANG, S., WU, J., WEINBERG, S. M., AND SHAPIRO, L. G. 2013. Improved detection of landmarks on 3D human face data. In *Engineering in Medicine and Biology Society (EMBC), 2013 35th Annual International Conference of the IEEE*, IEEE, 6482–6485.

MARCUS, L. F. 1996. *Advances in morphometrics*, vol. 284. Springer Science & Business Media.

MEYER, M., DESBRUN, M., SCHRÖDER, P., AND BARR, A. H. 2003. Discrete differential-geometry operators for triangulated 2-manifolds. In *Visualization and mathematics III*. Springer, 35–57.

NAIR, P., AND CAVALLARO, A. 2009. 3-D face detection, landmark localization, and registration using a point distribution model. *Multimedia, IEEE Transactions on 11*, 4, 611–623.

NEESER, R., ACKERMANN, R. R., AND GAIN, J. 2009. Comparing the accuracy and precision of three techniques used for estimating missing landmarks when reconstructing fossil hominin crania. *American journal of physical anthropology 140*, 1, 1–18.

PAGENDARM, H.-G., AND POST, F. H. 1995. Comparative visualization-approaches and examples.

PARULEK, J., TURKAY, C., REUTER, N., AND VIOLA, I. 2012. Implicit surfaces for interactive graph based cavity analysis of molecular simulations. In *Biological Data Visualization (BioVis), 2012 IEEE Symposium on*, IEEE, 115–122.

PERAKIS, P., PASSALIS, G., THEOHARIS, T., AND KAKADIARIS, I. A. 2011. 3D facial landmark detection & face registration. *University of Athens, Tech. Rep., January*.

RATHOD, D., VINAY, A., SHYLAJA, S., AND NATARAJAN, S. 2014. Facial landmark localization – a literature survey.

ROHLF, F. J., AND SLICE, D. 1990. Extensions of the procrustes method for the optimal superimposition of landmarks. *Systematic Biology 39*, 1, 40–59.

RUIZ, M. C., AND ILLINGWORTH, J. 2008. Automatic landmarking of faces in 3D – ALF^{3D}. In *Visual Information Engineering, 2008. VIE 2008. 5th International Conference on*, IET, 41–46.

SEGUNDO, M. P., QUEIROLO, C., BELLON, O. R. P., AND SILVA, L. 2007. Automatic 3D facial segmentation and landmark detection. In *Image Analysis and Processing, 2007. ICIAP 2007. 14th International Conference on*, IEEE, 431–436.

SOILLE, P. 2003. *Morphological image analysis: Principles and Applications*, vyd. 1. ed. Springer Verlag, Berlin, 204–206.

VEZZETTI, E., MARCOLIN, F., AND STOLA, V. 2013. 3D human face soft tissues landmarking method: an advanced approach. *Computers in Industry 64*, 9, 1326–1354.

WEISSTEIN, E. W. Osculating circle. MathWorld – A Wolfram Web Resource. http://mathworld.wolfram.com/OsculatingCircle.html. Accessed: 2015-02-14.

WHITMARSH, T., VELTKAMP, R. C., SPAGNUOLO, M., MARINI, S., AND TER HAAR, F. 2006. Landmark detection on 3D face scans by facial model registration. In *1st international symposium on shapes and semantics*, Citeseer, 71–75.

ZHANG, L., RAZDAN, A., FARIN, G., FEMIANI, J., BAE, M., AND LOCKWOOD, C. 2006. 3D face authentication and recognition based on bilateral symmetry analysis. *The Visual Computer 22*, 1, 43–55.